Al-Rafidain Engineering Journal (AREJ) Vol. 29, No. 2, September 2024, pp. 111-118

DCNN For Cataract Disease Detection Based on Model Parallelism

Mamoon A Al Jbaar * **Shefa A. Dawwd****
mamoon.thanoon@uoninevah.edu.iq shefa.dawwd@uomosul.edu.iq

* Department of Computer and Information Engineering, College of Electronics Engineering, Ninevah University, Mosul, Iraq
** Department of Computer Engineering, College of Engineering, University of Mosul, Mosul, Iraq

Received: February 24th, 2024 Received in revised form: March 20th, 2024 Accepted: April 5th, 2024

ABSTRACT

The retina is susceptible to numerous diseases, and cataracts are most prevalent, especially in developing nations. Cataracts are recognized as one of the most impactful diseases affecting the retina, given their propensity to develop asymptomatically and potentially lead to blindness or impaired vision among the elderly. Timely detection of cataracts and appropriate intervention is pivotal in mitigating disease progression and reducing instances of blindness attributable to this condition. This study provides a deep learning system based on parallel architectures, that utilized a proposed deep convolutional neural network (DCNN), to detect and diagnose cataract disease accurately. ODIR dataset was used for training and validating the proposed model, which achieved 97.7% accuracy for cataract detection, with an inference time of no more than 0.06 sec.

Keywords:
Cataract; Deep learning; Inference; Ocular; CNN.

1. INTRODUCTION

Recently, there has been an increase in the number of eye diseases, especially with the widespread use of advanced devices and means, such as tablets, mobile phones, and others [1]. These diseases contrast in their effects on vision, some of which lead to permanent blindness if left untreated, while other cases, like cataracts, glaucoma, Hypertension, blurred vision, and the like, contribute to varying degrees of visual impairment [2]. Early diagnosis plays an essential role in reducing the effects of these diseases and their side effects on the eye, it leads to identifying the pathological condition and accelerating its treatment [3].The huge gap between the number of specialized medical staff in the field of Ophthalmology and the increasing number of cases of eye diseases poses a serious challenge, and prevents the provision of necessary medical services to a large part of these patients, especially in rural areas[4]. Moreover, the diagnosis of eye diseases based on fundus images requires advanced medical experience as well as it needs time for diagnosis. Hence, the importance of using computer-aided systems based on artificial intelligence to detect and diagnose eye diseases automatically, leading to a reduction in both time and medical efforts [5]. Many studies and research works have dealt with the diagnosis of ocular diseases through proposed intelligent systems, where in [6] Ling lin et al. introduced a cataract detection framework, based on CNN. The proposed model utilized 5620 images collected from Beijing Tongren Eye Center of Beijing Tongren Hospital, for training and validation. through the evaluation phase, the model achieved 93% accuracy in the cataract detection process. In [7] Ramgopal et at. presented a deep-learning model for glaucoma detection. The presented model mainly consists of two phases the segmentation phase to segment the optic cup and the feature extraction phase, wherein in the first one a pre-trained transfer learning was integrated with the UNet deep learning network, while the function of phase two is accomplished through DenseNet-201 deep network. The model was trained and tested based on a glaucoma dataset of 650 images, where the model achieved about 96.90% in the testing process. In addition, Diabetic Retinopathy was efficiently detected and classified through the model proposed by Usharani et al. in [8]. The suggested model utilizes ResNet-152 as a pre-trained deep network for feature extraction from the input images, with an enhanced activation function. each of DIARETDB0, DRIVE, CHASE, and Kaggle datasets was exploited for training and testing the presented model, which achieved 99.41% accuracy with the Kaggle dataset. Moreover, ResNet-50 is utilized in [9] by Rui Fan et al, for detecting Ocular Hypertension. The proposed model was trained based on a dataset of 66,715 images and achieved a detection accuracy of about 95 %. In [10] Jen Hong Tan et al. presented a deep-learning model based on the proposed CNN network for detecting Age-related Macular Degeneration ocular disease. The proposed CNN, which consists of 14 layers, is trained based on a dataset collected from KMC Medical College in India. the proposed model showed high efficiency with detecting accuracy reaching 95.45%. Nomura et al [11], introduced Myopia deep learning detection system. The researchers relied on a presented CNN for feature extraction and classification through training based on the PALM challenge 2019 dataset. The proposed model achieved a detection accuracy of up to 95%.

In addition to this introduction, this paper contains four other sections. Section 2 presents the theoretical basis of the work. The proposed methodology is fully explained in section 3. The obtained results and their corresponding discussions are included in section 4. Finally, section 5 concludes this paper.

2. THE THEORETICAL BASES

This research work adopts the principle of model parallelism, which provides for splitting the model's architectural structure into a set of sections that work in parallel with each other to simplify the implementation of the model, to reduce its complexity, and increase its speed [12]. Thus, the architecture of the proposed deep network for cataract diagnosis has been implemented in a parallel approach, where each convolution and maxpooling processes were fragmented into eight sub-processes running concurrently with each other. Equation 1 represents the concurrent eight feature maps extracted through the parallel paths, while Equation 2 shows the final output based on aggregated features for the overall parallel pathways.

$$X(w+1)_{abc} = \sum_{w=0}^{7} (B_{wc} + \sum_{i=1}^{n} \sum_{j=1}^{m} \sum_{z=1}^{d} K_{0ijzc}.X_{a+i-1,b+j-1,z}) \ldots\ldots..(1)$$

$$Final\ out = \sigma(X1_{abc} // X2_{abc} // X3_{abc} // X4_{abc} \ldots\ldots\ldots // X8_{abc}) \ldots\ldots\ldots(2)$$

K_{0ijzc} ….., K_{7ijzc} , are the eight parallel kernels In the parallel paths within channel c, X represented the input to the parallel branches. $B(w+1)$, are the bais in eight pathways within channel c. Finally, i, j, z are the input dimensions. After that, the final out is exploited by the classifier to identify whether the fundus image has cataract disease or not.

3. THE PROPOSED METHODOLOGY

Far from the adoption of large-scale pre-training deep networks, the experimental work involves proposing a new Deep Learning Network with a limited size, finite number of learning parameters, and high efficiency to detect and diagnose cataracts.

The proposed model aims to be implemented in an inexpensive, low-power consumption environment, so the proposed architecture is implemented according to the adoption of the model parallelism approach. Model parallelization involves the fragmentation of the internal architecture of the deep network into multiple mini-clusters that can work in parallel and synchronously with each other on a set of multiprocessing modules.

3.1 Dataset

ODIR comprises a structured ophthalmic database containing data from 5,000 patients, encompassing information from both eyes. The dataset comprises age details, color fundus photographs from both the left and right eyes, and diagnostic keywords provided by medical professionals. Curated by Shang gong Medical Technology Co., Ltd., this dataset mirrors real-world patient information sourced from diverse hospitals and medical centers across China [13]. Fundus images in the database were captured using various commercially available cameras, including Canon, Zeiss, and Kowa, resulting in images with varying resolutions. Fig. 1 shows samples ODIR dataset [14].

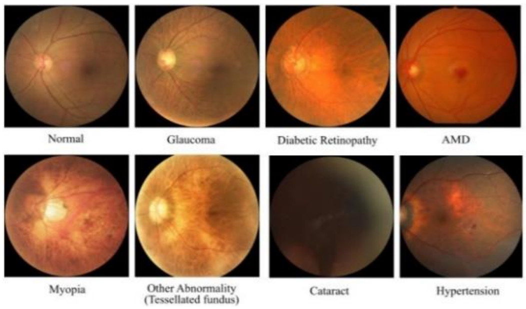

Fig. 1 ODIR image samples [14].

3.2 Data pre-processing

However, the dataset presents several challenges, particularly due to numerous poorly lighted and unclear photographs, this is due to the variety and variety of hardware sources providing images. Consequently, pre-processing is imperative before employing them as inputs in the proposed system. Typically, many researchers resort to exploit various pre-processing methods, like Standardization, Normalization, Histogram equalization, Feature scaling, and others. The main aim of the pre-processing is to improve the quality of data, as well as enhance the system performance [15]. Histogram equalization stands as a simplified image processing technique to enhance the quality of images, it is used for contrast improvement and to optimize the feature extraction process. Histogram equalization can adapt to varied lighting conditions, leading to standardized intensity distribution across images. These advantages help CNNs better distinguish between different features in an image, making it easier to extract meaningful patterns and information during the training process, besides contributing to the generalization of the CNN model [16]. As we have already noted earlier, histogram equalization is used as a pretreatment to enhance the efficiency of the presented system and improve some images in the dataset, which is used for training and testing the proposed deep learning network, It improved the results at the level of accuracy of the model performance by 3%. Figure 2 shows the impact of preprocessing on database models.

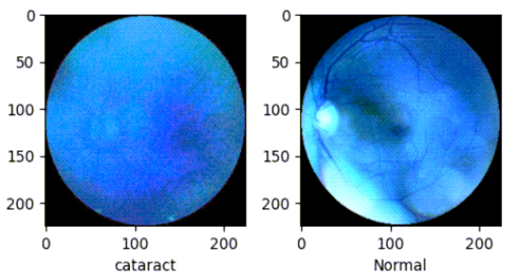

Fig. 2 Impact of Histogram equalization on image

3.3 Cataract dataset extracting and preparing

The ODIR dataset involves multiple ocular diseases, like Cataracts, Glaucoma, Hypertension, Moderate nonproliferative retinopathy, Age-related Macular Degeneration, Myopia, and Others. This dataset also has data annotation, which is represented by the image's label, patient age, diagnostic information provided by ophthalmologists, etc. as shown in Fig. 3. The data annotations are utilized for segregating the cataract images and their normal cases from the ODIR dataset and constructing the training and testing dataset for the cataract detection process.

ID	Right-Fundus	Left-Diagnosti	Right-Diagnostic K	N	D	G	C	A	H	M	O	labels	target
21	21_right.jpg	epiretinal me	epiretinal membra	0	0	0	0	0	0	0	1	['O']	[0, 0, 0, 0, 0, 0, 0, 1]
23	23_right.jpg	hypertensive_	hypertensive_reti	0	0	0	0	0	1	0	0	['H']	[0, 0, 0, 0, 0, 1, 0, 0]
24	24_right.jpg	normal fundu	cataract	0	0	0	1	0	0	0	0	['C']	[0, 0, 0, 1, 0, 0, 0, 0]
26	26_right.jpg	moderate_no	moderate_non_pr	0	1	0	0	0	0	0	1	['D']	[0, 1, 0, 0, 0, 0, 0, 0]
27	27_right.jpg	normal fundu	macular epiretina	0	1	0	0	0	0	0	1	['O']	[0, 0, 0, 0, 0, 0, 0, 1]
28	28_right.jpg	hypertensive_	hypertensive_reti	0	0	0	0	0	1	0	0	['H']	[0, 0, 0, 0, 0, 1, 0, 0]
29	29_right.jpg	epiretinal me	normal fundus	0	0	0	0	0	0	0	1	['N']	[1, 0, 0, 0, 0, 0, 0, 0]
31	31_right.jpg	epiretinal me	normal fundus	0	0	0	0	0	0	0	1	['N']	[1, 0, 0, 0, 0, 0, 0, 0]
32	32_right.jpg	hypertensive_	hypertensive_reti	0	0	0	0	0	1	0	0	['H']	[0, 0, 0, 0, 0, 1, 0, 0]
33	33_right.jpg	normal fundu	macular epiretina	0	0	0	0	0	0	0	1	['O']	[0, 0, 0, 0, 0, 0, 0, 1]
34	34_right.jpg	drusen	drusen	0	0	0	0	0	0	0	1	['O']	[0, 0, 0, 0, 0, 0, 0, 1]
35	35_right.jpg	pathological r	normal fundus	0	0	0	0	0	0	1	0	['N']	[1, 0, 0, 0, 0, 0, 0, 0]
37	37_right.jpg	macular epire	normal fundus	0	1	0	0	0	0	0	1	['N']	[1, 0, 0, 0, 0, 0, 0, 0]
38	38_right.jpg	macular hole	normal fundus	0	0	0	0	0	0	0	1	['N']	[1, 0, 0, 0, 0, 0, 0, 0]
40	40_right.jpg	macular epire	macular epiretina	0	0	0	0	0	0	0	1	['O']	[0, 0, 0, 0, 0, 0, 0, 1]
42	42_right.jpg	normal fundu	epiretinal membra	0	0	0	0	0	0	0	1	['O']	[0, 0, 0, 0, 0, 0, 0, 1]
43	43_right.jpg	wet age_relat	dry_age_related_r	0	0	1	0	1	0	0	0	['A']	[0, 0, 0, 0, 1, 0, 0, 0]

Fig. 3 Dataset annotations.

3.4 The proposed deep network.

A limited-size deep network has been proposed that emulates VGG16 network in its architecture, but it is smaller in size and less in terms of the number of learning parameters, this is because VGG16 network is characterized by simplicity, depth, effective feature extraction, transfer learning capabilities, and empirical performance. The proposed network consists of eight successive convolution layers interspersed with four Maxpooling layers to identify the most prominent features among the convolution layers. Where the first two convolutional layers utilize 64 kernels of 3x3, as well as the ReLU activation function, to ensure that the output has the same input value if it is positive; otherwise, the output is zero. This is followed by the maxpooling layer, which selects the most prominent features among the set of features produced by the convolution layers and also contributes to reducing feature map dimensionality.

Figure 4 shows the original VGG16 Net as well as the proposed network's architectural structure and the details of each layer.

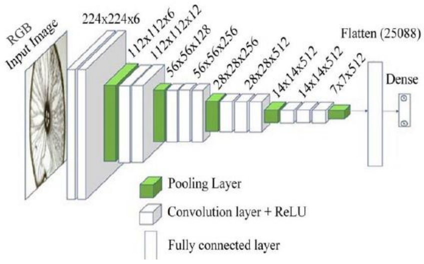

(a)

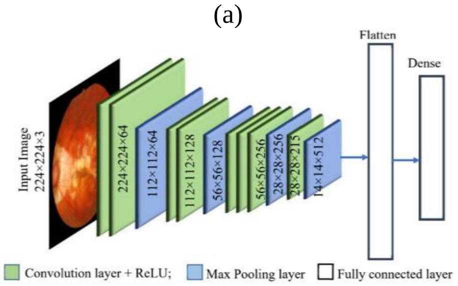

(b)

Layer	Output shap3	Parameter#
Conv2D_1	(None,224,224,64)	1,792
Conv2D_2	(None,224,224,64)	36,928
MaxPooling2D	(None,112,112,64)	0
Conv2D_3	(None,112,112,128)	73,856
Conv2D_4	(None,112,112,128)	147,584
MaxPooling2D	(None,56,56,128)	0
Conv2D_5	(None,56,56,256)	295,168
Conv2D_6	(None,56,56,256)	590,080
Conv2D_7	(None,56,56,256)	590,080
MaxPooling2D	(None,28,28,256)	0
Conv2D_8	(None,28,28,512)	1,180,160
MaxPooling2D	(None,14,14,512)	0
Flatten	(None,100352)	0
Dense	(None,1)	100,353
Total parameters	3,016,001	
Trainable parameters	3,016,001	
Non- Trainable parameters	0	

(c)

Fig4 a- The Original VGG16, b- Proposed deep Network, c- layers details of the proposed network

Fig. 4(c) refers to the details of each convolution and maxpooling layers that construct the proposed deep network, where the figure shows the dimensions as well as the learning parameters for each layer. The figure also refers to differences in the total number of training parameters of the network between the proposed network and the original VGG16, where it does not exceed 3,016,001 parameters, and it a very few if compared to those in other deep learning networks such as VGG16 networks, whose training parameters reach 14,915,400 for the same number of output classes, and is almost five times this number, as well as the Inception-V3, and ResNet-50, which their training parameters are 222,123,92, and 24,390,536 respectively. The number of training parameters of the proposed deep network and its small size reflect the low complexity of the network, in addition to its fast response.

Wherein Equation 3 computes the overall operation (GFLOPS) within the deep network.

$$GFLOP\ total = \sum_{j=0}^{m} Ops(j) + D_{Ops} \ \ldots..(3)$$

Where: D_{Ops} means the dense layer operations, m denotes the number of convolutional layers, and *Ops(j)* represents the total number of operations in (j) convolutional layer, which is calculated through Equation (4) [17, 18]

$$Ops = I/P\ ch \times O/P\ ch \times K_H \times K_W \times O/P_H \times O/P_W \ldots\ldots.(4)$$

Where: I/P ch and O/P ch represented the number of input channels (or features) and output channels (or features), respectively, where K_H, K_W, and O/P_H, O/P_W express the dimensionality of convolution kernel the output after padding, respectively. So, the overall GFLOPS in the proposed network does not exceed 10.26002125, which is less than those in VGG16 by 1.5X.

3.5 Parallel implementation of deep network based on Model Parallelism

As we noted in the previous section, the small size of the proposed deep network, in addition to the reduction in the amount of computations within the network, motivated the adoption of a parallel architecture to implement the proposed network architecture. Model parallelism is considered the best way to manage large and complex models, as this type of parallelism is concerned with dividing the model into parts that can work simultaneously with each other on several processing units. This approach can be translated into deep learning fields and neural networks, where model parallelism can be emulated by dividing a deep model or neural network with significant parameters and many layers into parallel parts that work simultaneously across several processing units. This type of parallelism leads to an optimal investment of available hardware resources like memory and multiple processing units and is suitable for platforms with limited resources, like embedded systems platforms.

The infrastructure of the proposed network is parallelized into 8 parallel paths that work concurrently with each other As clarified in Fig. 5.

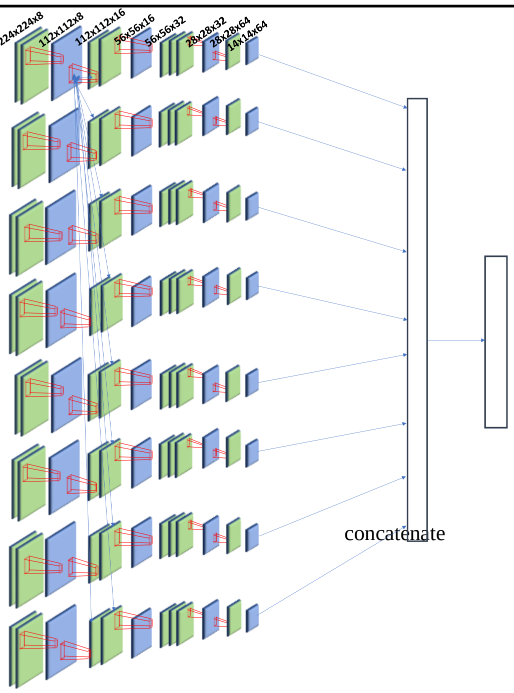

In this Fig only layer1 interconnection was noted to maintain the clarity of the figure.

Fig. 5 Parallel infrastructure of the proposed deep network

As shown in Fig.5, the whole architecture of the proposed network is implemented in a parallel scheme within eight concurrent paths. So that all Convolution and Maxpooling layers in the deep network are implemented in parallel and synchronous paths. The presented architecture targeted multi-core processing units as well as the limited resource platforms. The compact size of the proposed network alongside its parallel implementation architectures streamlined the training process and simplified the network's complexity, computations, and ease of deployment across diverse parallel environments, irrespective of resource constraints. Additionally, the parallel implementation of the network architecture aided in diminishing response time and augmenting the number of calculations per second. Notably, the overall inference time of the model was measured at 0.06 seconds, while the GFLOPS/s (GigaFLOPS per second) reached 171, within the colab environment that was utilized for training and evaluating the presented model.

3.6 Model training

The 1094 cataract/normal images, in the ODIR dataset which was split as 80:20 for training and validation, where the model was trained for 70 epochs, and optimized using Adam Optimizer, and the learning rate of learning rate =0.0001.

4. RESULTS AND DISCUSSIONS

The most famous criteria were used in evaluating the performance of the presented deep system, which are Accuracy, Precision, Recall, and F1-score. The accuracy can be calculated based on Equation 5.

$$Accuracy = \frac{TP + TN}{TP + TN + FP + FN} \dots..(5)$$

Where *TP*, *TN* represent True Positive, and True Negative respectively, while FP is a False Positive, and *FN* False Negative. Fig. 6 explains the accuracy and loss of the proposed model.

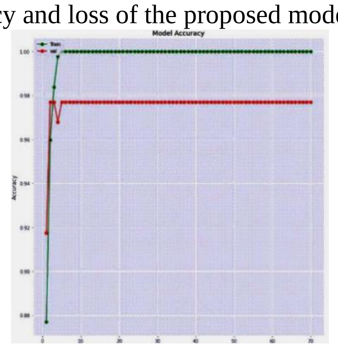

(a)

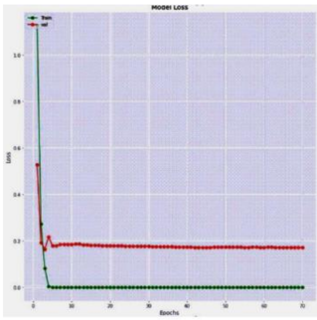

(b)

Fig 6 Accuracy and Loss of the Proposed Model (a) training/validation accuracy; (b) training/validation loss.

Also, Equation 6, presents the calculation of the Precision metric.

$$Precision = \frac{TP}{TP + FP} \dots \dots \dots..(6)$$

While the Recall metric can be computed through Equation 7.

$$Recall = \frac{TP}{TP + FN} \dots \dots \dots..(7)$$

The final metric F1-Score, which combines both precision and recall of a classifier into a singular value, is computed relying on Equation 8.

$$F1 - Score = 2 * \frac{Precision * Recall}{Precision + Recall} \dots..(8)$$

Table 1 summarizes the values of the evaluation criteria for the proposed model.

Table1:Evaluation metric for the proposed model

Variable	Precision	Recall	F1-Score	Accuracy
0	1	0.95	0.98	0.977
1	0.96	1	0.98	

In addition, and for completing the evaluation process for the presented model, Fig. 7 shows the model's confusion matrix.

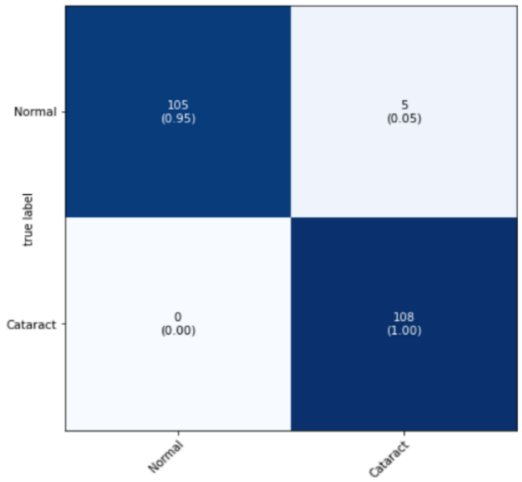

Fig 7 Model's confusion matrix

From Table 1, the high precision reflects the model's ability to precisely identify relevant instances from the overall instances, while a high recall value of the proposed model demonstrates that the model has a low false negative rate. Finally, a high F1-score denotes that the model effectively balances between minimizing false positives and false negatives.

The combination of all evaluation metrics gives a comprehensive view of the performance of the proposed model and its efficiency in diagnosing a cataract disease, where the proposed model achieved high levels in all performance evaluation criteria.

4.1 Model's performance comparsion

After the performance evaluation of the proposed parallel model, it is necessary to compare it with other systems that have been trained and tested using the same database, and this is shown in Table 2, which involves a set of research works for detecting and diagnosing cataract disease using deep learning systems.

Table 2: Model performance comparison

Paper	Deep model	Accuracy
G. Sharma et al. [19], 2023	ResNet50	90%
P. Singh et al. [20], 2023	Light wiegt deep network	95.8%
Y. Elloumi et al. [21], 2022	CataractEyeNet	96.78%
A. Mangla et al. [22], 2022	CNN Model	93%
Y. Elloumi et al. [23], 2021	MobileNet-V2	90.68%
J. Ran et al. [24], 2018	CNN Model	90.69%, six level of cataract
P. K. Jha et al. [25], 2018	CNN Model	94.56%
Proposed parallel Model	**DCNN Model**	**97.7%**

Table 2 indicates the superiority of the proposed model over the rest of the models presented earlier, despite its limited size compared to those systems. Therefore, the proposed model can be described as a highly efficient model in detecting and diagnosing cataract disease that can be adapted to provide the necessary medical support to specialized medical personnel.

5. CONCLUSION

Despite its limited size, the proposed deep network for cataract diagnosis has proven to be as efficient as the pre-trained deep networks, such as VGG16, ResNet, and others. In addition, the parallel implementation of the proposed network architecture contributed to reducing the complexity of the network and simplifying its computations, which helped to speed up the network training process and reduce the inference time in general.

Since the proposed deep network architecture is intended for implementation in a resource-limited environment, it is possible to deploy the proposed system on low-cost edge platforms such as the Jetson and IoT platforms, as an embedded system with limited power consumption.

ACKNOWLEDGEMENTS

The researchers would like to extend their thanks and appreciation to Mosul University/College of Engineering/Computer Engineering department for their support, which has assisted in boosting the outcomes of this research paper.

REFERENCES

[1] G. Alwakid, W. Gouda, and M. Humayun, "Deep Learning-based prediction of Diabetic Retinopathy using CLAHE and ESRGAN for Enhancement,"

in Healthcare, 2023, vol. 11, no. 6: MDPI, p. 863 DOI: 10.3390/healthcare11060863

[2] A. A. Marouf, M. M. Mottalib, R. Alhajj, J. Rokne, and O. Jafarullah, "An efficient approach to predict eye diseases from symptoms using machine learning and ranker-based feature selection methods," *Bioengineering*, vol. 10, no. 1, p. 25, 2022. https://doi.org/10.3390/bioengineering10010025

[3] S. Albahli and G. N. Ahmad Hassan Yar, "Automated detection of diabetic retinopathy using custom convolutional neural network," *Journal of X-Ray Science and Technology*, vol. 30, no. 2, pp. 275-291, 2022.

[4] F. Demir and B. Taşcı, "An effective and robust approach based on R-CNN+ LSTM model and ncar feature selection for ophthalmological disease detection from fundus images," *Journal of Personalized Medicine*, vol. 11, no. 12, p. 1276, 2021.

[5] K. N. Alam et al., "Deep learning-based sentiment analysis of COVID-19 vaccination responses from Twitter data," *Computational and Mathematical Methods in Medicine*, vol. 2021, 202. https://doi.org/10.1155/2021/4321131

[6] L. Zhang, J. Li, H. Han, B. Liu, J. Yang, and Q. Wang, "Automatic cataract detection and grading using deep convolutional neural network," *in 2017 IEEE 14th international conference on networking, sensing and control (ICNSC)*, 2017: IEEE, pp. 60-65. doi: 10.1109/ICNSC.2017.8000068.

[7] R. Kashyap, R. Nair, S. M. P. Gangadharan, M. Botto-Tobar, S. Farooq, and A. Rizwan, "Glaucoma detection and classification using improved U-Net Deep Learning Model," *in Healthcare*, 2022, vol. 10, no. 12: MDPI, p. 2497. https://doi.org/10.3390/healthcare10122497

[8] U. Bhimavarapu and G. Battineni, "Deep Learning for the Detection and Classification of Diabetic Retinopathy with an Improved Activation Function," *in Healthcare*, 2022, vol. 11, no. 1: MDPI, p. 97. https://doi.org/10.3390%2Fhealthcare11010097

[9] R. Fan *et al.*, "Detecting glaucoma in the ocular hypertension study using deep learning," *JAMA ophthalmology*, vol. 140, no. 4, pp. 383-391, 2022.

[10] J. H. Tan *et al.*, "Age-related macular degeneration detection using deep convolutional neural network," *Future Generation Computer Systems*, vol. 87, pp. 127-135, 2018. https://doi.org/10.1016/j.future.2018.05.001

[11] N. Rauf, S. O. Gilani, and A. Waris, "Automatic detection of pathological myopia using machine learning," *Scientific Reports*, vol. 11, no. 1, p. 16570, 2021. https://doi.org/10.1038/s41598-021-95205-1

[12] M. Yan, N. Meisburger, T. Medini, and A. Shrivastava, "Distributed slide: Enabling training large neural networks on low bandwidth and simple cpu-clusters via model parallelism and sparsity," *arXiv preprint arXiv:2201.12667*, 2022. https://doi.org/10.48550/arXiv.2201.12667

[13] J. Lin, Q. Cai, and M. Lin, "Multi-label classification of fundus images with graph convolutional network and self-supervised learning," *IEEE Signal Processing Letters*, vol. 28, pp. 454-458, 2021.

[14] G. Seif, "Handling imbalanced datasets in deep learning," Retrieved August, vol. 8, p. 2020, 2018.

[15] L. A. Zanlorensi, E. Luz, R. Laroca, A. S. Britto, L. S. Oliveira, and D. Menotti, "The impact of preprocessing on deep representations for iris recognition on unconstrained environments," in *2018 31st SIBGRAPI conference on graphics, patterns and images (SIBGRAPI)*, 2018: IEEE, pp. 289-296.

[16] J. David Freire, J. Rodrigo Montenegro, H. Andres Mejia, F. Paul Guzman, C. Enrique Bustamante, R. Xavier Velastegui, et al. 2021 4th International Conference on Data Storage and Data Engineering 2021 Pages: 45-51.

[17] H. Kim, H. Nam, W. Jung, and J. Lee, "Performance analysis of CNN frameworks for GPUs," in 2017 IEEE International Symposium on Performance Analysis of Systems and Software (ISPASS), 2017: IEEE, pp. 55-64.

[18] K. Guo, S. Zeng, J. Yu, Y. Wang, and H. Yang, "[DL] A survey of FPGA-based neural network inference accelerators," ACM Transactions on Reconfigurable Technology and Systems (TRETS), vol. 12, no. 1, pp. 1-26, 2019.

[19] G. Sharma, V. Anand, and S. Gupta, "Harnessing the Strength of ResNet50 to Improve the Ocular Disease Recognition," in *2023 World Conference on Communication & Computing (WCONF)*, 2023: IEEE, pp. 1-7.

[20] P. Singh, B. Naveen, A. R. Mohapatra, B. Annappa, and S. Dodia, "Light-weight Deep Learning Model for Cataract Detection using Novel Activation Function," in *2023 14th International Conference on Computing Communication and Networking Technologies (ICCCNT)*, 2023: IEEE, pp. 1-6.

[21] A. Sohail, H. Qayyum, F. Hassan, and A. U. Rahman, "CataractEyeNet: A Novel Deep Learning Approach to Detect Eye Cataract Disorder," in *Proceedings of International Conference on Information Technology and Applications: ICITA 2022*, 2023: Springer, pp. 63-75.

[22] A. Mangla, S. Dhall, N. Gupta, S. Rastogi, and S. Yadav, "Ocular Disease Recognition Using Convolutional Neural Networks," in *International Advanced Computing Conference*, 2022: Springer, pp. 422-433.

[23] Y. Elloumi, "Mobile aided system of deep-learning based cataract grading from fundus images," in *Artificial Intelligence in Medicine: 19th International Conference on Artificial Intelligence in Medicine, AIME 2021, Virtual Event, June 15–18, 2021, Proceedings*, 2021: Springer, pp. 355-360.

[24] J. Ran, K. Niu, Z. He, H. Zhang, and H. Song, "Cataract detection and grading based on combination of deep convolutional neural network

and random forests," in *2018 international conference on network infrastructure and digital content (IC-NIDC)*, 2018: IEEE, pp. 155-159. http://dx.doi.org/10.1109/ICNIDC.2018.8525852

[25] P. K. Jha and A. Verma, "Fundus Image Classification using Quantized Deep Learning," 2018.

نظام الكشف عن مرض اعتام العدسة باستخدام الشبكة العميقة المنفذة باعتماد نهج توازي النموذج

مأمون عبد الجبار ذنون*
mamoon.thanoon@uoninevah.edu.iq

شفاء عبد الرحمن داؤود**
shefa.dawwd@uomosul.edu.iq

*قسم هندسة الحاسوب والمعلوماتية، كلية هندسة الالكترونيات، جامعة نينوى، موصل، العراق
**قسم هندسة الحاسوب، كلية الهندسة، جامعة الموصل، موصل، العراق

تاريخ الاستلام:24 فبراير 2024 استلم بصيغته المنقحة: 20 مارس 2024 تاريخ القبول :5 ابريل 2024

الملخص

تكون شبكية العين عرضة للعديد من الأمراض ، ومن ابرزها مرض اعتام عدسة العين, فهو الأكثر انتشارا وخاصة في الدول النامية. يتم تعريف إعتام عدسة العين كواحد من أكثر الأمراض التي تؤثر على شبكية العين ، نظرا لميلها إلى التطور بدون أعراض وربما يؤدي إلى العمى أو ضعف البصر بين كبار السن. يعد الكشف في الوقت المناسب عن إعتام عدسة العين والتدخل المناسب أمرا محوريا في التخفيف من تطور المرض وتقليل حالات العمى التي تعزى إلى هذه الحالة. توفر هذه الدراسة نظام التعلم العميق القائم على أساس المعماريات المتوازية ، لكشف وتشخيص مرض اعتام العدسة بدقة . تم استخدام مجموعة بيانات أودير للتدريب والتحقق من صحة النموذج المقترح ، والذي حقق دقة 97٪ للكشف عن إعتام عدسة العين ، مع وقت الاستدلال لا يزيد عن 0.06 ثانية .

الكلمات الداله :
اعتام العدسة، التعلم العميق، الاستدلال، العين الشبكة العصبية التلافيفية.